Retina Publish Ahead of Print
DOI: 10.1097/IAE.0000000000004811

Ellipsoid zone integrity at angiographic leak following resolution of central serous chorioretinopathy : MICRoN report number Two

Nasiq Hasan MD[1] , Arman Zarnegar MD[2], Hosein Nouri[3,4], Stanley Saju DO[5], Jessica Cao MD[5], Avery Zhou MD[5], Charles Wykoff MD, PhD[5], Priya Shah BS[6], Panisa Singhanetr MD[6], Elizabeth J Rossin MD, PhD[6], Lorenzo Ferro Desideri MD, PhD[8], Felicia Hertkorn MD[9], Marion R Munk MD, PhD[7,8,9], Stela Vujosevic[10], Lisa Checchin MD[11], Lorenzo Pili MD[11], Maurizio Battaglia Parodi MD[12], Carmen Antia MS[13], Luis Arias Barquet MD, PhD [13], Michael Zhang[14,15], Yusuf Ashfaq BS[16], Zachary Kroeger MD[16], Min Kim MD, PhD, MBA[17], Lihteh Wu MD[18], Jay Chhablani MD[1,2], Macula society International CSCR Research Network – MICRoN

Affliations

[1]University of Pittsburgh Medical Center, Pittsburgh, PA, USA

[2]University of Pittsburgh School of Medicine, Pittsburgh, PA, USA

[3]School of Medicine, Isfahan University of Medical Sciences, Isfahan, Iran

[4]Ophthalmic Research Center, Research Institute for Ophthalmology and Vision Science, Shahid Beheshti University of Medical Sciences, Tehran, Iran

[5]Retina Consultants of Texas, Retina Consultants of America, Blanton Eye Institute, Houston Methodist Hospital, Houston, TX, USA

[6]Harvard Medical School Department of Ophthalmology within Massachusetts Eye and Ear (MEE), Boston, MA

[7]Department of Ophthalmology, Northwestern University Feinberg School of Medicine, Chicago, IL, USA

[8]Inselspital, University Hospital Bern, Bern, Switzerland

[9]Gutblick, Pfäffikon, Switzerland

[10]Department of Biomedical, Surgical and Dental Sciences, University of Milan, Milan, Italy;

[11]Eye Clinic, IRCCS MultiMedica, Milan, Italy.

[12] Department of Ophthalmology, Vita-Salute San Raffaele University, Ospedale San Raffaele, Milan, Italy.

[13]Department of Ophthalmology, Hospital Universitari de Bellvitge, Carrer de La Feixa Llarga, S/N, 08907, L'Hospitalet de Llobregat, Catalunya, Spain.

[14]The Canberra Hospital, Yamba Dr, Garran ACT 2605, Australia

[15]Sydney and Sydney Eye Hospital, 8 Macquarie St, Sydney NSW 200, Australia

[16]Casey Eye Institute at Oregon Health and Science University, 515 SW Campus Dr., Portland, OR

[17]Yonsei University College of Medicine, 211 Eonjuro, Gangnam-gu, Seoul, 06273, Republic of Korea.

[18]Asociados de Macula Vitreo y Retina de Costa Rica, San José, Costa Rica

Running head: EZ integrity in CSCR

Corresponding author

Jay Chhablani, MD

5.631, 1622, Locust street

Department of Ophthalmology

University of Pittsburgh Medical Center , Vision Institute

chhablanijk2@upmc.edu

jay.chhablani@gmail.com

Funding and Support
No funding was received from the NIH, Wellcome Trust, or Howard Hughes Medical Institute.

Proprietary Interest Statement
The authors declare no proprietary or commercial interest in any product or concept discussed in this article.

Key words: Central serous chorioretinopathy, Ellipsoid zone, Fluorescein angiography, Optical coherence tomography

Summary statement: Significant proportion of patients with resolved central serous chorioretinopathy (CSCR) do not regain optimal vision, potentially due to the development of atrophic ellipsoid zone. In this study we found that longer symptom duration, complex CSCR and irregular photoreceptor outer segment thickening are associated with increased risk of EZ atrophy.

Abstract

Purpose–This study aimed to explore prognostic factors for predicting ellipsoid zone integrity and its association with angiographic leakage and OCT biomarkers at baseline

Methods – In this multicentre retrospective study resolved CSCR eyes with perifoveal angiographic leak at baseline were included. Baseline demographics, clinical features, and anonymized imaging data, including fluorescein angiography, and OCT were collected. The leakage site was identified on FA, and its corresponding location on OCT was analyzed for structural changes and photoreceptor outer segment elongation. CMT, SFCT, Haller's layer thickness (HLT), and Haller's index (HLT/SFCT) were measured at baseline and follow-up. EZ integrity following resolution was classified as continuous, discontinuous and atrophic.

Results– Eighty four eyes with resolved CSCR were included. Longer symptom duration (p=0.032) and complex CSCR (p=0.04), were associated with a higher likelihood of atrophic EZ. Significant reductions in CMT, SFCT, and HLT were observed in all groups, whereas Haller's index significantly reduced only in continuous EZ. Multinominal regression showed significant association between complex CSCR and atrophic EZ.

Conclusion– Longer symptom duration, complex CSCR and irregular PROS thickening are associated with increased risk of EZ atrophy in resolved CSCR. Identifying these risk factors early may help predict visual outcomes and guide patient counselling.

Introduction

Central serous chorioretinopathy (CSCR) primarily affects the choroid and retinal pigment epithelium (RPE). It is characterized by a serous neurosensory retinal detachment (NSRD) and pigment epithelial detachment (PED). The primary pathophysiology is thought to involve thickened, hyperpermeable choroidal vessels leading to leakage of fluid across the RPE into the subretinal space along with other cardinal characteristics including a thickened sclera.[1,2] Leakage of fluid across the RPE can be visualized using fluorescein angiography (FA) as hyperfluorescent leaks, which is broadly classified as inkblot and smokestack leaks.[3] Identifying the location of these leaks is important as they primarily guide treatment planning particularly for cases requiring focal laser, PDT or subthreshold laser. Strategized treatment, particularly in chronic or persistent cases of CSCR minimizes photoreceptor damage and prevent further vision loss.

In recent years, new biomarkers across various imaging modalities have emerged, with optical coherence tomography (OCT) being particularly important.[4] OCT is often performed as a standalone imaging modality for patients with acute CSCR helping to detect structural features including NSRD, serous PED, double layer sign (DLS),[5] dipping sign,[6] vacuole sign,[7] elongation of photoreceptor outer segment (PROS) and its associated thinning near leak sites. For chronic CSCR, OCT is commonly used in conjunction with FA, indocyanine green angiography (ICGA) and fundus autofluorescence (FAF) to assess fluid persistence, resolution, photoreceptor and RPE integrity, and choroidal parameters. OCT changes corresponding to areas of hyperfluorescent leaks on FA and hyperfluorescent plaques on ICGA have been previously studied.[8] The potential of OCT to replace FA and ICG has been debated, though it is known to complement it effectively. A study by Maltsev

et al. highlighted the use of OCT in identifying leakage points in CSCR.[9] Another study proved that enhanced depth imaging (EDI) and swept source-OCT (SS-OCT) reliably identified the hyperfluorescent lesions on ICGA.[8] Enhanced detection of signs on OCT and accurate leak localization could potentially reduce the reliance on invasive techniques like FA and ICGA and mitigate the associated risks. However, the diagnostic yield of FA and ICGA in CSCR remains high and the risk of adverse events are extremely rare, and therefore, OCT may only complement traditional angiography at present.

Treatment is often deferred in cases of acute CSCR with a single leakage point, minimal RPE changes, and non-severe symptoms, given the high probability of spontaneous SRF resolution in the first 4 months.[10] However, persistent SRF can still damage photoreceptors even at early stages, and the longer it persists, the greater the risk of irreversible photoreceptor insult.[11] Previous research has documented elongation of PROS and associated morphologic changes overlying the SRF.[12] Our prior study had also demonstrated thinning of PROS near leakage sites.[13] A recent study demonstrated that the elongation of PROS negatively correlate with visual acuity in acute and active CSCR.[14] However, the morphology of the ellipsoid zone (EZ), which corresponds to PROS in resolved CSCR, has not been thoroughly investigated. EZ integrity is closely associated with visual function, but it cannot be accurately assessed while the neurosensory retina is detached. EZ integrity in resolved CSCR can be influenced by various factors, including demographics, CSCR duration, treatment methods, structural changes on OCT, and leakage pattern in the active phase. For example, many patients with prolonged SRF may exhibit varying degree of EZ attenuation and visual impairment post-resolution.[1516] Despite its importance, the nature of EZ alterations and whether patients at higher risk of EZ atrophy could be identified remain incompletely understood. This study aimed to explore the prognostic potential of

demographic, structural and angiographic features for predicting EZ integrity at the site of leakage, as well as describe the OCT changes observed at the leakage point.

Methods

Setting and approval

This multicenter, retrospective study was conducted as a part of the Macula Society International CSCR Research Network (MICRoN) and adhered to the tenets of the Declaration of Helsinki. Institutional Review Board (IRB) approval was obtained from all participating centers, with a waiver of informed consent granted due to the minimal-risk and retrospective nature of the study. Data sharing agreements among collaborators and the procedures for demographic, clinical, and imaging data collection and analysis have been detailed in prior publications of the project.[17] All images were meticulously analyzed by an experienced retina specialist (NH) and 10% of the sample images were independently reviewed and validated by another masked grader (AZ) to ensure accuracy and consistency. In case of disagreements, the measurements and segmentations were adjudicated by the senior author (JC)

Inclusion criteria, clinical information and definitions

Of the entire dataset provided by collaborators, patients with active, first episode CSCR who had perifoveal leak (within 6mm diameter from the centre of the fovea) at baseline FA and resolved SRF at follow up were included; eyes were excluded from the analysis if there was no active leak on FA, if the leak was outside the perifoveal area on FA and when the NSD was non-foveal. The minimum duration between baseline and follow up was 4 months. All images were reviewed by the contributing authors to verify the accuracy of

the diagnosis and the absence of a secondary choroidal neovascularisation (CNV), and any eyes were excluded if the diagnosis of CSCR was found to be incorrect or a secondary CNV was found to be present. (see Figure 1, Supplemental Digital Content 1, which demonstrates inclusion and exclusion of cases). Serial OCT volumes were analysed and presence of recurrence in between visits or persistent fluid at final follow up were excluded. Collected data included age at baseline, gender, systemic comorbidities, and systemic steroid use. Snellen's best-recorded visual acuity (BRVA) at baseline and follow-up was converted to Logarithm of the Minimum Angle of Resolution (LogMAR). The duration of symptoms before presentation was measured in weeks and duration between baseline and final visit was measured in months. CSCR was classified as simple or complex based on RPE changes observed in AF or IR images. Simple CSCR was defined as having a single area of RPE alteration not exceeding 2 disc areas. [18]

Quantitative analysis of OCT

An experienced grader (NH) evaluated the OCT data and manually measured central macular thickness (CMT), subfoveal choroidal thickness (SFCT), NSRD height, and subfoveal Haller's layer thickness (HLT) which has been previously explained in a prior publication from the group. [17] . Subfoveal Haller's index was calculated as the ratio of HLT to total choroidal thickness. Inter-class coefficient was calculated between the masked graders (NH and AZ) for thickness measurements including CMT, SFCT, HLT and lesions (NSRD height, PED height) of randomly selected 10% of the OCT volumes from the cohort.

Qualitative analysis of FA and OCT

FA leaks were classified into four types based on appearance: dense inkblot, smudge inkblot and smoke stack pattern and a newly identified type termed "spray" leaks. Spray leaks

initially start as a single focal point of leak during the early phase and then spread horizontally (unlike smoke stack leaks, which exhibit vertical dye diffusion) with increasing area and intensity (Figure 2). At baseline, the area on the OCT that corresponded to active leaks on the FA was traced topographically using the IR image and the same location was identified at follow up OCT scans using the toggle icon on these registered OCT volumes. The mapping of OCT regions to FA leaks was performed based on the earliest hyperfluorescent frame in FA.

OCT biomarkers at the site of leakage were identified, including PED/DLS, subretinal fibrin, dipping sign (outward traction of neurosensory retina by subretinal fibrin), hypertransmission tail (area of increased OCT signal transmission into the choroid through a defect of the RPE), vacuole sign (hyporeflective lucency surrounded by hyperreflective subretinal fibrin), and dimple sign (local thinning of the elongated PROS; see Figure 3). PROS elongation was classified as uniform, irregular, and irregularly speckled.

Patients with any episode of recurrence were excluded from analysis. Following SRF resolution, the EZ (hyperreflective line immediately underlying the external limiting membrane) at the point of original leak was mapped (using baseline FA and OCT; see Figure 4 and 5) and analyzed. Participants were grouped based on EZ integrity at the leakage site upon their follow-up visit into: i) continuous, ii) discontinuous, and iii) atrophic (absence of hyperreflective line). Continuous EZ referred to a single line with uniform thickness EZ without any intervening disruptions in its continuity. Discontinuous EZ referred to a single line with intervening disruptions in the continuity of EZ. Atrophic EZ showed complete absence of EZ. These three groups were compared in terms of their demographics, visual acuity, FA leakage pattern, quantitative and qualitative OCT biomarkers, and treatment modality.

Statistics

Statistical analysis was performed using SPSS statistical software version 23 (SPSS Inc., Chicago, IL, USA). Categorical variables were expressed by frequency and percentage and continuous ones by mean (standard deviation; SD) or median (interquartile range; IQR) depending on the normality of distribution as assessed by the Shapiro-Wilk test. For intergroup comparisons, we used ANOVA with Bonferroni post-hoc (for parametric data) or Kruskal Wallis (for nonparametric data). Chi-square tests were used to analyze categorical variables among groups. When the Chi-square test result was not significant but cross-tabulations suggested a pattern of relationship, adjusted standardized residuals were calculated to identify specific deviations. .[19] An absolute value of the adjusted standardized residual greater than 1.96 was considered significant, with positive values indicating positive deviations and negative values indicating negative deviations Paired t-test and Wilcoxon signed-rank test were used to compare baseline and follow up data with and without normal distribution, respectively. Parameters that were significant on univariate logistic regression were considered for multinomial logistic regression. A p-value of less than 0.05 was considered statistically significant.

Results

The current study included 84 eyes of 80 patients of which 30 (35.7%) had continuous EZ, 28 (33.3%) had discontinuous EZ, and 26 had atrophic EZ (30.9%). Mean age of this cohort was 44.25 ±11.04 years, with 65 (73%) being male. Bilateral CSCR was found in 19 patients (23%) based on clinical data and imaging findings, however only 4 patients exhibited bilateral active leaks and were included in the study. Other baseline characteristics are

outlined in Table 1. The most common comorbidity was hypertension 21 (25%) followed by systemic steroid exposure 15 (18%). The atrophic group had significantly longer duration of symptoms (p=0.032). Most patients with simple CSCR had continuous EZ at follow-up visits, while those with complex CSCR were more likely to have an atrophic EZ (p=0.04). For the 10% of volumes that were analysed by a masked second grader (AZ) the ICC was 0.97 (95% CI: 0.95-0.98, p<0.001).

At baseline, the included eyes had a mean BRVA of 0.29 ±0.26 logMAR (20/40) and was similar among the three groups (p=0.398). CMT, and SFCT were 416.06 ±179.89 microns, and 398.24 ±113.07 respectively. No intergroup differences were noted regarding baseline CMT, SFCT, NSRD height, Haller's layer thickness, or Haller's index. Analysis of fluorescein leak type and EZ integrity revealed overall significance (χ^2=12.922,p=0.044), and adjusted standardized residuals suggested that dense inkblot leaks were more frequent than expected in continuous EZ group (ASR=2.2) and less so in atrophic EZ group (ASR=-2.3). In contrast, smudge inkblot leaks were less common in continuous EZ group (ASR=-2.5). With respect to baseline structural markers, none of them reached significant associations on Chi-square test, however adjusted standardized variables showed that PED/DLS (χ^2=5.397, p= 0.067:ASR= -2.3), dipping sign (χ^2=5.669, p= 0.059:ASR= -2.4) and uniform PROS (χ^2=7.843, p= 0.097:ASR=-2.4) were less frequent in eyes with atrophic EZ, whereas irregular speckled PROS (χ^2=7.843, p= 0.097:ASR= 2.6) were more common in this group.

The median follow up duration was around 35 months and was similar among the three groups (0.648). At baseline, mean BRVA was similar between the groups. However, at follow up, BRVA was significantly worse in patients with atrophic EZ compared to those with continuous and discontinuous EZ (Continuous group:0.096 ±0.19 logMAR units

(20/25), discontinuous group :0.099 ±0.12 logMAR units (20/25) and atrophic group : 0.25±0.32 logMAR units (20/36) (p=0.047), but the difference was not significant between continuous and discontinuous EZ groups. Overall, BRVA improvement was significant in eyes with continuous and discontinuous EZ, unlike in those with atrophic EZ post-resolution. Mean CMT, SFCT and Haller's layer thickness were reduced from baseline to post resolution, overall and across all groups. Although no overall reduction was noted in the Haller's index, a significant decrease was evident only in eyes with continuous EZ (p=0.037). Comparison of baseline and follow-up parameters are presented in Table 2. Multinomial logistic regression showed a significant association between complex CSCR and atrophic EZ post resolution. (Table 3)

Discussion

In the current study, continuous EZ integrity at resolution was more frequently observed in patients with simple CSCR at baseline, whereas atrophic EZ was more common in those with complex CSCR. Dense inkblot leaks were more common and smudge inkblots were less common among patients with continuous EZ. There was significant improvement in BRVA and reduction of CMT, SFCT and Haller's layer thickness from baseline to post resolution among all patients and the continuous and discontinuous groups, however BRVA did not change significantly in the atrophic EZ group. BRVA was notably worse in patients with atrophic EZ at follow up compared to continuous and discontinuous EZ. The Haller's index did not change significantly in discontinuous and atrophic group but reduced significantly in the continuous EZ group.

FA remains the gold standard for classifying and accurately localizing leaks in CSCR, and together with ICG it is primarily used to guide treatments such as focal laser, PDT and subthreshold laser.[20] We hypothesize that different types of leaks can affect the photoreceptors differently. Dense inkblots and smudge inkblots were classified based on the intensity of leak and regularity of the border of leak in the late stage of the FA. Thinning of elongated photoreceptors at the point of leak has been previously demonstrated.[13] However, assessing the disruption of photoreceptors is challenging unless the SRF has resolved. We identified three types of EZ morphology upon resolution: continuous EZ, discontinuous EZ and atrophic EZ. Various OCT biomarkers have been established in the literature.[4] PED and DLS were the most common biomarker at the point of leak, with DLS typically being smaller (less than 1000 microns) than previously defined.[21] We hypothesize that the DLS may start as a PED and flatten out over time as fluid egresses.

Previous literature has linked EZ integrity with visual prognosis after CSCR resolution. Failure to improve vision post-resolution may relate to photoreceptor disruption.[15] In our study, we observed that dense inkblot leaks were more frequently associated with continuous EZ status, while smudge inkblots were more common in the atrophic EZ group. Smudge inkblot leaks may occur in patients with pre-existing RPE alterations, where scarred RPE impedes the continuous egress of fluid, resulting in less intense and more irregular leak patterns.[22] Atrophic EZ was associated with longer symptom duration and complex CSCR, likely due to earlier disruption of the RPE and overlying photoreceptors from prolonged fluid exposure. Patients with simple CSCR generally had intact photoreceptors, evident as continuous EZ at resolution. Additionally, irregularly speckled PROS at baseline were more prevalent in the atrophic EZ group. These speckles corresponding to hyperreflective dots in the outer retinal layers which indicate severe, irreparable photoreceptor damage that does not

regenerate after resolution, leading to EZ atrophy.[23] As expected, the BRVA was poorer in atrophic EZ and did not significantly improve post-resolution.

Analysis of OCT parameters at baseline and follow up revealed significant reductions in CMT, SFCT and HLT at the fovea. The Haller's index did not change significantly in the entire study cohort, indicating similar thinning across choroidal layers. However, in patients with continuous EZ, the Haller's index was significantly reduced suggesting that the thickness of the inner choroidal layers did not change significantly. This may imply that the maintenance of inner choroidal morphology (choriocapillaris and Sattler's layer) is crucial for preserving photoreceptor integrity. Gujar et al have also reported that abnormal perfusion of choriocapillaris affects the integrity of the overlying photoreceptors using in vivo visualization of photoreceptors with high magnification module in CSCR and correlating the findings with OCTA and OCT.[24]

Our study had several limitations, including the need for a larger sample size to accurately demonstrate the associations between leak types and photoreceptor health. It would have helped us to adjust or stratify the outcomes based on treatment options as modalities such as laser and PDT can alter the architecture of RPE and EZ per se. As this study includes multicenter data, variations in data entry methods and imaging modalities may introduce inconsistency which could affect the uniformity of collected data. However as all images were read and analysed in a single center by two trained retina specialists, this inconsistency was effectively addressed. EZ architecture, assessed at the leak site would not directly correlate with the foveal EZ architecture or the visual acuity. However, we have included leaks that are within the 6 mm diameter centered on the fovea to assess how different leaks may impact photoreceptor structure and contribute to variations in the

morphology of the EZ band following resolution. Long-term follow-up is necessary to assess further photoreceptor degradation or regeneration over time, because photoreceptor stress, and thus EZ discontinuity, may not have subsided immediately after resolution. However, we considered only cases with foveal neurosensory detachment. Measurements were performed manually by a single experienced grader and only 10% of the images were reviewed by a second specialist.

This study identifies specific associations between different types of CSCR leaks (such as dense inkblot and smokestack leaks) and biomarkers of photoreceptor health, such as EZ integrity and photoreceptor elongation. It emphasizes that different leak types impact photoreceptor health differently, with dense inkblot leaks often linked to preserved photoreceptors (continuous EZ), while atrophic EZ is more common in cases of complex CSCR. Predicting photoreceptor damage in acute CSCR is crucial for assessing potential visual impairment or deterioration that may ensue. Given that observation is the primary management strategy for acute CSCR, merely observing these cases, as is done for most cases, may not suffice and active management during the acute stages may be necessary to prevent permanent photoreceptor damage.

Supplemental Digital Content 1-http://links.lww.com/IAE/C892

Appendix 1-http://links.lww.com/IAE/C893

References

1. Kanda P, Gupta A, Gottlieb C, et al. Pathophysiology of central serous chorioretinopathy: a literature review with quality assessment. *Eye*. 2022;36(5):941-962. doi:10.1038/s41433-021-01808-3

2. Zarnegar A, Ong J, Matsyaraja T, et al. Pathomechanisms in central serous chorioretinopathy: A recent update. *Int J Retina Vitr*. 2023;9:3. doi:10.1186/s40942-023-00443-2

3. Yamada K, Hayasaka S, Setogawa T. Fluorescein-angiographic patterns in patients with central serous chorioretinopathy at the initial visit. *Ophthalmol J Int Ophtalmol Int J Ophthalmol Z Augenheilkd*. 1992;205(2):69-76. doi:10.1159/000310315

4. Nkrumah G, Paez-Escamilla M, Singh SR, et al. Biomarkers for central serous chorioretinopathy. *Ther Adv Ophthalmol*. 2020;12:2515841420950846. doi:10.1177/2515841420950846

5. Yang L, Jonas JB, Wei W. Optical coherence tomography-assisted enhanced depth imaging of central serous chorioretinopathy. *Invest Ophthalmol Vis Sci*. 2013;54(7):4659-4665. doi:10.1167/iovs.12-10991

6. Kim HC, Cho WB, Chung H. Morphologic Changes in Acute Central Serous Chorioretinopathy Using Spectral Domain Optical Coherence Tomography. *Korean J Ophthalmol KJO*. 2012;26(5):347-354. doi:10.3341/kjo.2012.26.5.347

7. Rajesh B, Kaur A, Giridhar A, Gopalakrishnan M. "VACUOLE" SIGN ADJACENT TO RETINAL PIGMENT EPITHELIAL DEFECTS ON SPECTRAL DOMAIN OPTICAL COHERENCE TOMOGRAPHY IN CENTRAL SEROUS CHORIORETINOPATHY ASSOCIATED WITH SUBRETINAL FIBRIN. *Retina Phila Pa*. 2017;37(2):316-324. doi:10.1097/IAE.0000000000001192

8. Munk MR, Shah R, Pappas F, et al. Multimodal Imaging and Choroidal Volumetric Changes After Half-fluence PDT in Central Serous Chorioretinopathy. *Curr Eye Res*. 2016;41(1):97-106. doi:10.3109/02713683.2014.1002047

9. Maltsev DS, Kulikov AN, Chhablani J. Topography-guided identification of leakage point in central serous chorioretinopathy: a base for fluorescein angiography-free focal laser photocoagulation. *Br J Ophthalmol*. 2018;102(9):1218-1225. doi:10.1136/bjophthalmol-2017-311338

10. Feenstra HMA, van Dijk EHC, Cheung CMG, et al. Central serous chorioretinopathy: An evidence-based treatment guideline. *Prog Retin Eye Res*. 2024;101:101236. doi:10.1016/j.preteyeres.2024.101236

11. Hata M, Oishi A, Shimozono M, et al. Early changes in foveal thickness in eyes with central serous chorioretinopathy. *Retina Phila Pa*. 2013;33(2):296-301. doi:10.1097/IAE.0b013e31826710a0

12. Matsumoto H, Kishi S, Otani T, Sato T. Elongation of photoreceptor outer segment in central serous chorioretinopathy. *Am J Ophthalmol*. 2008;145(1):162-168. doi:10.1016/j.ajo.2007.08.024

13. Maltsev DS, Kulikov AN, Burnasheva MA, Chhablani J. Photoreceptor outer segment layer thinning as a biomarker in acute central serous chorioretinopathy. *Ther Adv Ophthalmol*. 2023;15:25158414231160689. doi:10.1177/25158414231160689

14. Ma J, Meng Nana, Xu X, et al. System review and meta-analysis on photodynamic therapy in central serous chorioretinopathy. *Acta Ophthalmol (Copenh)*. 2014;92(8). doi:10.1111/aos.12482

15. Fujita A, Aoyama Y, Tsuneyoshi S, et al. Association between visual function and the integrity of residual ellipsoid zone in resolved central serous chorioretinopathy. *Sci Rep*. 2019;9(1):12433. doi:10.1038/s41598-019-48825-7

16. Singh SR, Iovino C, Zur D, et al. Central serous chorioretinopathy imaging biomarkers. *Br J Ophthalmol*. 2022;106(4):553-558. doi:10.1136/bjophthalmol-2020-317422

17. Hasan N, Zarnegar A, Jacob N, et al. Clinical Characteristics and Progression of Pachychoroid Macular Atrophy in Central Serous Chorioretinopathy. *Ophthalmol Retina*. Published online April 11, 2025. doi:10.1016/j.oret.2025.04.005

18. Chhablani J, Cohen FB, Aymard P, et al. Multimodal Imaging-Based Central Serous Chorioretinopathy Classification. *Ophthalmol Retina*. 2020;4(11):1043-1046. doi:10.1016/j.oret.2020.07.026

19. Naioti E, Mudrak E. Using Adjusted Standardized Residuals for Interpreting Contingency Tables.

20. Daruich A, Matet A, Dirani A, et al. Central serous chorioretinopathy: Recent findings and new physiopathology hypothesis. *Prog Retin Eye Res*. 2015;48:82-118. doi:10.1016/j.preteyeres.2015.05.003

21. Kim YH, Kang E, Oh J. Factors related to the location of pigment epithelial detachment in central serous chorioretinopathy. *Sci Rep*. 2022;12:4507. doi:10.1038/s41598-022-08550-0

22. Nicholson B, Noble J, Forooghian F, Meyerle C. Central Serous Chorioretinopathy: Update on Pathophysiology and Treatment. *Surv Ophthalmol*. 2013;58(2):103-126. doi:10.1016/j.survophthal.2012.07.004

23. Jhaveri A, Melo IM, Pecaku A, et al. Outer Retinal Hyperreflective Dots: A Potential Imaging Biomarker in Rhegmatogenous Retinal Detachment. *Ophthalmol Retina*. 2023;7(12):1087-1096. doi:10.1016/j.oret.2023.07.016

24. Gujar R, Muzi A, Cagini C, et al. In-vivo visualization of the photoreceptors using Spectralis High Magnification Module imaging in central serous chorioretinopathy. *Am J Ophthalmol Case Rep*. 2022;25:101249. doi:10.1016/j.ajoc.2021.101249

Figure Legends

Figure 1: Angiography images of different types of leaks at early and late phases. Dense inkblot leak (A,B), Smudge inkblot leak (C,D), Smokestack leak (E,F) and Spray leak. (G,H)

Figure 2: OCT Biomarkers at point of leak. A- OCT shows a small DLS with a dimple at the PROS layer and fibrin in the SRF. B- OCT shows a characteristic vacuole sign (white arrow) over the DLS with surrounding fibrin, C – OCT shows a hypertransmission tail (white arrow) in the choroid nasal to the DLS with an overlying dimple in the PROS, D –OCT shows a small DLS with dipping (of the outer retinal layers) sign (grey arrow) and minimal fibrin, E– OCT shows dipping sign, PED and vertical fibrin material in the SRF. F-H shows different types of PROS elongation on OCT. F – uniform, G - irregular and H - irregular speckled

Figure 3: Topographical mapping of OCT biomarkers at leak site. A – FA showing point of leak (yellow arrow) at early phase. B – Tracing of leak on baseline OCT using corresponding IR image. OCT shows DLS and fibrin at leak point. C- Automated localization of leakage point using the next icon (red arrow) on HEYEX – 2 interface. OCT shows atrophic EZ at leak point

Figure 4: Topographical mapping of OCT biomarkers at leak site. A – FA showing point of leak (white arrow). B – Tracing of leak on baseline OCT using corresponding IR image. OCT shows DLS and fibrin at leak point and vacuole sign. C- Automated localization of leakage point using the next icon (black arrow) on HEYEX – 2 interface. OCT shows continuous EZ at leak

Figure 5: Topographical mapping of OCT biomarkers at leak site. A – FA showing point of leak (white arrow) at early phase. B – Tracing of leak on baseline OCT using corresponding IR image. OCT shows DLS at leak point. C- Automated localization of leakage point using the next icon (black arrow) on HEYEX – 2 interface. OCT shows discontinuous EZ at leak

Supplemental file Figure 1: Flowchart showing inclusion of patients in the study

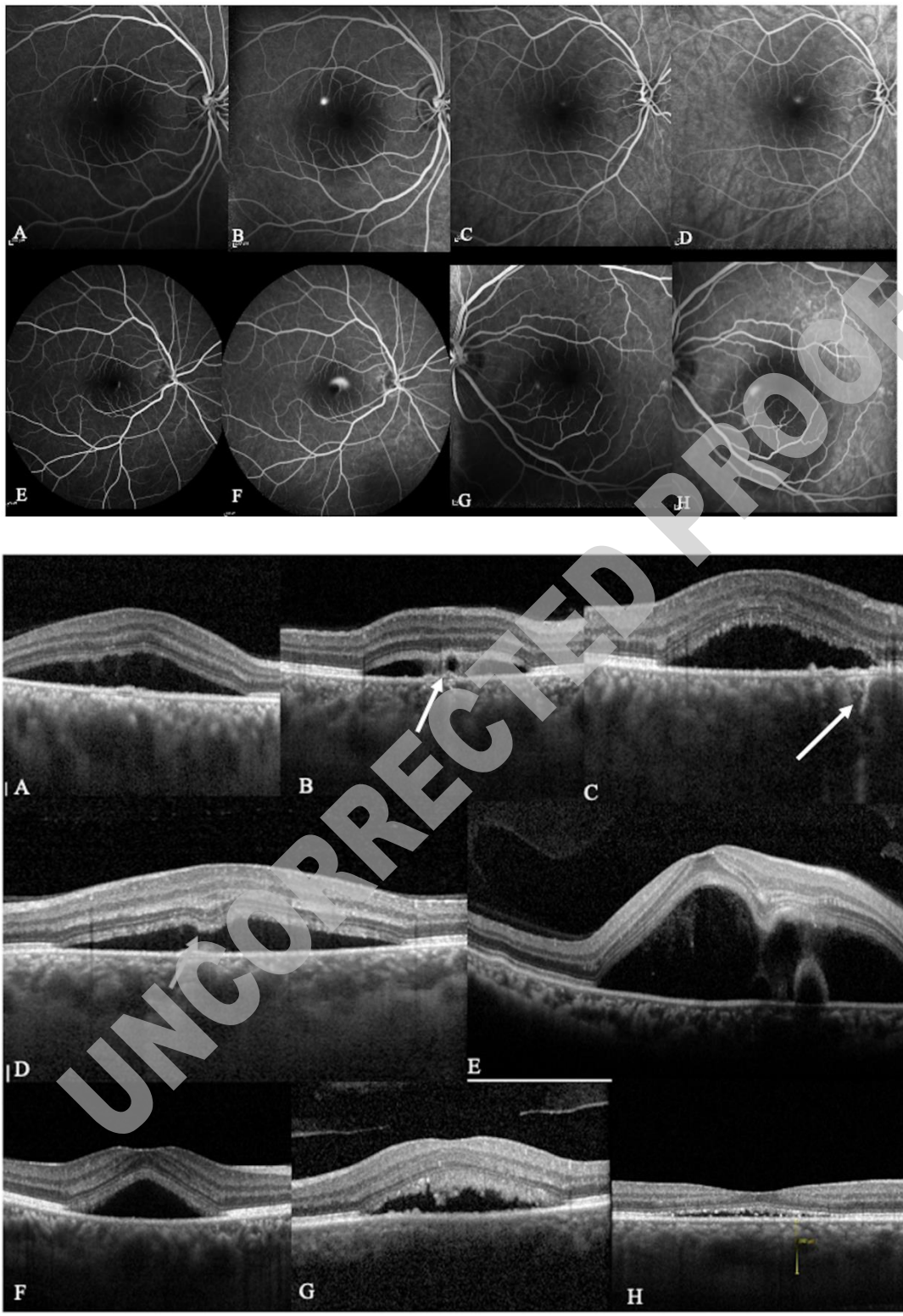

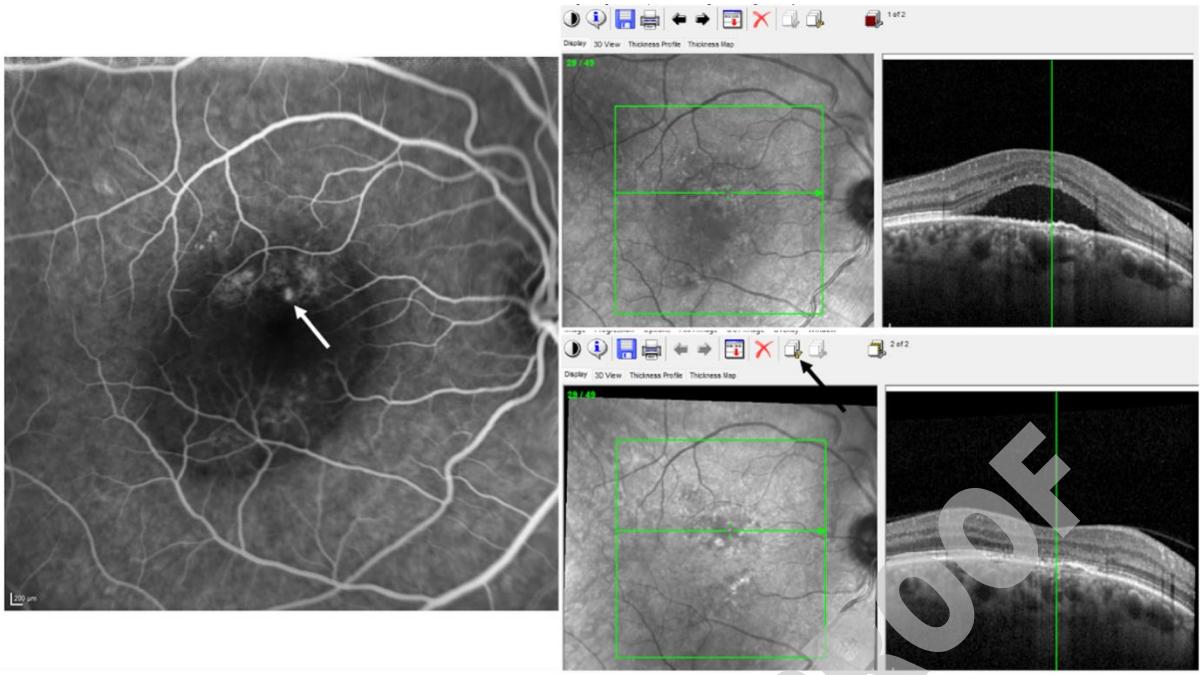

		Grouped by EZ integrity				
		Overall (n=84)	Continuous EZ (n=30)	Discontinuous EZ (n=28)	Atrophic EZ (n=26)	P - value
Age (years)		44.25±11.04	41.57±8.97	46.06±13.04	45.38±10.69	0.25
Gender (males), n (%)		65 (73%)	22 (73%)	20 (71%)	23 (88%)	0.119
Laterality, n (%)	Unilateral	65 (73%)	23 (76%)	22 (79%)	20 (77%)	0.983
	Bilateral	19 (23%)	7 (23%)	6 (21%)	6 (23%)	0.983
Duration of symptoms (weeks)		4 (2.625 -24.5)	4 (2.5-17)	4 (2.25-16)	7 (4-49.5)	**0.032**
Simple CSCR, n (%)		52 (62%)	21 (70%)	19 (68%)	12 (46%)	**0.04**
Duration of follow up, months (median, IQR)		35.41 (8.27-68.82)	33.94 (7.28-62.84)	45.63 (5.43 - 81.45)	39.55 (14.54-75.61)	0.648
Hypertension, n (%)		21 (25%)	8 (27%)	6 (21%)	7 (27%)	0.867
Steroid intake, n (%)		15 (18%)	5 (17%)	4 (14%)	6 (23%)	0.685
Treatment	Observation	42 (50%)	17 (57%)	14 (50%)	11 (42%)	0.92
	Focal laser	2 (2%)	0 (0%)	1 (4%)	1 (4%)	
	PDT	5 (6%)	2 (7%)	2 (7%)	1 (4%)	
	Subthreshold laser	25 (30%)	8 (27%)	8 (29%)	9 (34%)	
	AntiVEGF	3 (4%)	1 (3%)	1 (4%)	1 (4%)	
	MCRA	3 (4%)	1 (3%)	0 (0%)	2 (8%)	
Baseline BRVA (logMAR)		0.29 ±0.28	0.34±0.35	0.24±0.21	0.28±0.26	0.398
Type of leak, n (%)	Dense inkblot	17 (20%)	10 (33%)	16 (57%)	1 (4%)	0.095
	Smudge inkblot	58 (69%)	16 (53%)	21 (75%)	21 (81%)	
	Spray	3 (4%)	1 (3%)	1 (4%)	1 (4%)	
	Smoke stack	6 (7%)	3 (10%)	0 (0%)	3 (12%)	
OCT Biomarkers	PED/DLS	75 (89%)	28 (93%)	27 (96%)	20 (77%)	0.067
	Fibrin	45 (54%)	15 (50%)	15 (54%)	15 (58%)	0.847
	Vacuole sign	16 (19%)	7 (23%)	3 (11%)	6 (23%)	0.388
	Dipping sign	16 (19%)	8 (27%)	7 (25%)	1 (4%)	0.059
	Dimple	17 (20%)	7 (23%)	5 (18%)	5 (19%)	0.864
	Hypertransmission tail	34 (40%)	11 (37%)	10 (36%)	13 (50%)	0.491
PR Elongation	Uniform	42 (50%)	18 (60%)	16 (57%)	8 (31%)	0.097
	Irregular	19 (23%)	6 (20%)	7 (25%)	6 (23%)	
	Irregularly speckled	23 (27%)	6 (20%)	5 (18%)	12 (46%)	
CMT		416.06 ±179.89	454.97 ±182.54	412.36 ± 136.16	375.15 ±212.57	0.254
SFCT		398.24 ±113.07	407.53 ±134.29	392.32 ± 90.979	393.88 ±111.48	0.856
NSD Height		233.51 ±171.38	243.62 ±144.92	221.36 ± 148.32	235.46 ±224.63	0.887
Haller's layer thickness		279.93 ±105.28	294.55 ±122.13	273.07 ± 86.67	270.64 ±105.28	0.642
Haller's index		0.69 ± 0.11	0.7±0.13	0.69± 0.09	0.67±0.1	0.576

Table 1 – Baseline characteristic of patients in the overall study and among three groups. CSCR- Central serous chorioretinopathy, PDT- Photodynamic therapy, VEGF – Vascular endothelial growth factor, MRA – Mineralocorticoid antagonist. BRVA – Best recorded visual acuity, PED – pigment epithelial detachment, DLS- double layer sign, PR-Photoreceptor, CMT – Central macular thickness, SFCT – subfoveal choroidal thickness, NSD – Neurosensory detachment

Parameters	Continuous EZ (n=30)			Discontinuous EZ (n=28)			Atrophic EZ (n=26)			Total (n=84)		
	Baseline	Follow up	p-value	Baseline	Follow up	p-value	Baseline	Follow up	p-value	Baseline	Follow up	p-value
BRVA (logMAR)	0.34 ± 0.35	0.096 ±0.19	**<0.001**	0.24 ± 0.21	0.099 ±0.12	**<0.001**	0.28 ±0.26	0.25 ± 0.32	0.386	0.29 ± 0.28	0.14 ± 0.23	**<0.001**
CMT	454.97 ±182.54	203.59 ± 37.22	**<0.001**	412.36 ±136.16	189.33 ±40.54	**<0.001**	375.15± 212.56	196.48± 41.64	**<0.001**	416.06 ± 179.89	196.64±39.68	**<0.001**
SFCT	407.53 ±134.29	370.45 ± 130.48	**0.044**	392.32 ±90.979	336.74±85.89	**0.001**	393.88± 111.48	349.68± 97.84	**0.036**	398.24 ±113.08	352.8±106.92	**<0.001**
HLT	294.55 ±122.13	254.38± 123.21	**0.029**	273.07±86.670	232.26±71.47	**0.003**	270.64±105.283	237.96± 81.12	**0.043**	279.93±105.283	241.51±93.93	**<0.001**
Haller's index	0.7±0.13	0.66± 0.11	**0.037**	0.69± 0.09	0.68± 0.09	0.436	0.67±0.1	0.67±0.1	0.491	0.69 ± 0.11	0.67± 0.1	0.278

Table 3 – Comparison of quantitative measures at baseline and follow up among the three groups

BRVA – Best-recoded visual acuity, CMT- Central macular thickness, SFCT – subfoveal choroidal thickness, HLT - Haller layer thickness

Covariate	Univariate Logistic regression		Multivariate logistic regression	
	Discontinuous EZ OR (95%CI, pvalue)	Atrophic EZ OR (95%CI, pvalue)	Discontinuous EZ OR (95%CI, pvalue)	Atrophic EZ OR (95%CI, pvalue)
Age	1.04 (0.99-1.09, 0.12)	1.04 (0.98-1.09, 0.18)		
Duration of symptoms	0.99 (0.98-1.02, 0.77)	**1.02 (1.001 - 1.037, 0.038)**	0.99 (0.98-1.01,0.73)	1.01 (0.99-1.03, 0.24)
Gender (Males)	0.91 (0.287 -2.87, 0.87)	4.364 (0.835 – 22.81, 0.08)		
Complex CSCR	1.105 (0.35-3.53, 0.87)	**3.58 (1.16-11.04, 0.026)**	0.86 (0.24-3.05,0.82)	**4.42 (1.06-18.44,0.042)**

Table 3: Multinominal logisitic regression analysis of covariates associated with atrophic EZ